

Complex Langevin Simulation of the SU(3) Spin Model with Nonzero Chemical Potential

F. Karsch and H. W. Wyld

Department of Physics, University of Illinois at Urbana-Champaign, Urbana, Illinois 61801

(Received 20 September 1985)

We study the effective three-dimensional SU(3) spin model with nonzero chemical potential. This model describes the strong-coupling, large-fermion-mass limit of QCD at finite temperature and baryon density. The results obtained with a complex Langevin algorithm are encouraging for a future simulation of QCD with nonzero chemical potential. The Langevin simulations converge even for large values of the chemical potential, and excellent agreement with exact solutions in the extreme strong-coupling ($\beta = 0$) limit has been found.

PACS numbers: 11.15.Ex, 05.50.+q

Only recently has it been possible to study the thermodynamics of non-Abelian gauge theories in the presence of dynamical fermions in large-scale Monte Carlo simulations.¹ These calculations gave first indications on the phase structure of QCD at finite temperature,¹⁻³ the mass dependence of the deconfinement and chiral transitions,² and the dependence on the number of flavors.³ For a quantitative understanding of the equation of state of strongly interacting matter, it would be of considerable interest to analyze the phase diagram of QCD in the whole temperature-chemical-potential (T - μ) plane. However, although the formalism for dealing with finite chemical potentials in lattice gauge theories has been developed,⁴ standard numerical simulation techniques are not applicable at $\mu \neq 0$. The reason is that for $\mu \neq 0$ the fermion determinant is complex and thus leads to a complex Euclidean action. [Here and in the following we are concerned with a SU(3) theory. In the case of SU(2) gauge theory the fermion determinant is real and exploratory simulations at nonzero μ have been performed.⁵] The integrand of the Euclidean path integral defining the partition function thus does not have an immediate probability interpretation.

It has been noticed by Parisi⁶ and Klauder⁷ that, while standard Monte Carlo techniques fail in the case of complex actions, it is still possible to write down a

Langevin equation. In the case of a real action, time averages computed from the Langevin equation converge to equilibrium averages computed from the path integral. However, not much is known about the convergence properties of the Langevin equation for complex actions and the conditions under which it will yield results equivalent to those computed from the equilibrium distribution of the Euclidean path integral. Nonetheless, this approach has recently attracted much attention⁸⁻¹¹ and has been tested in the case of some simple models with complex actions which could be compared with exact solutions. These results are encouraging and show that at least for "not too large" contributions of the imaginary part in the action the Langevin equation will still resemble the distribution of the Euclidean path integral.

In the present Letter we will study the suitability of the complex Langevin algorithm for a simulation of QCD at finite chemical potential. As a preliminary step in this direction, we study the effective three-dimensional SU(3) spin model,¹²⁻¹⁴ which approximates the full SU(3) gauge theory with fermions in the strong-coupling, large-fermion-mass limit.

The partition function is given by

$$Z = \int \prod_x dU_x e^{-S}, \quad (1)$$

with action

$$S = -\beta \sum_{x,l} (\text{Tr} U_x \text{Tr} U_{x+l}^\dagger + \text{Tr} U_x^\dagger \text{Tr} U_{x+l}) - h \sum_x (e^\mu \text{Tr} U_x + e^{-\mu} \text{Tr} U_x^\dagger). \quad (2)$$

Here $U_x \in \text{SU}(3)$, μ is the chemical potential, and β and h are effective couplings related to the original parameters g^2 , T , and m (fermion mass) of the full gauge theory.

At $\mu = 0$ this model has been analyzed by use of mean-field techniques, and the phase structure in the temperature-mass plane has been studied.¹²⁻¹⁴ It has been found that the model has a line of first-order phase transitions in the (β, h) plane starting at $(0.13, 0)$ and ending in a second-order phase transition at $(\beta_c, h_c) = (0.12, 0.059)$.¹⁴ (In the heavy-fermion-mass limit the external-field parameter h can be related to the fermion mass, $h \sim e^{-m}$, while β is related to the bare coupling g^2 and T , $\beta \sim T$.) For $\mu \neq 0$ the action, Eq. (2), is complex. We may separate the imaginary part in the action by introducing the new couplings

$$\hat{h} = h \cosh \mu, \quad \hat{g} = h \sinh \mu. \quad (3)$$

The action then reads

$$S = -\beta \sum_{x,l} (\text{Tr} U_x \text{Tr} U_{x+l}^\dagger + \text{Tr} U_x^\dagger \text{Tr} U_{x+l}) - 2\hat{h} \sum_x \text{Re} \text{Tr} U_x - 2i\hat{g} \sum_x \text{Im} \text{Tr} U_x. \quad (4)$$

TABLE I. Comparison of results for $\langle \text{Tr}U \rangle$ and $\langle \text{Tr}U^{-1} \rangle$ at $\beta=0$ obtained from a Langevin simulation with a discrete time step $\epsilon = 0.005$ with exact results.

| h | μ | $\langle \text{Tr}U \rangle$ | | $\langle \text{Tr}U^{-1} \rangle$ | |
|-----|-------|------------------------------|--------|-----------------------------------|--------|
| | | Langevin | Exact | Langevin | Exact |
| 0.1 | 0.0 | 0.1089(24) | 0.1050 | 0.1089(24) | 0.1050 |
| | 0.5 | 0.0907(14) | 0.0742 | 0.1815(10) | 0.1667 |
| | 1.0 | 0.0763(50) | 0.0735 | 0.2736(43) | 0.2723 |
| | 1.5 | 0.1297(45) | 0.1217 | 0.4515(39) | 0.4467 |
| | 2.0 | 0.2807(72) | 0.2769 | 0.7268(32) | 0.7271 |
| | 2.5 | 0.6533(93) | 0.6548 | 1.1331(56) | 1.1404 |
| 1.0 | 0.0 | 1.2682(38) | 1.2676 | 1.2682(38) | 1.2676 |
| | 0.2 | 1.2633(41) | 1.2578 | 1.3441(34) | 1.3401 |
| | 0.4 | 1.3226(47) | 1.3162 | 1.4645(35) | 1.4613 |
| | 0.6 | 1.4401(28) | 1.4364 | 1.6120(21) | 1.6119 |
| | 0.8 | 1.5989(31) | 1.5986 | 1.7695(25) | 1.7725 |
| | 1.0 | 1.7774(22) | 1.7771 | 1.9264(10) | 1.9287 |

The phase diagram at $\mu \neq 0$ has been analyzed in the mean-field approach for the case where the fields U_x are restricted to the $Z(3)$ center of the $SU(3)$ group.¹⁵ There it has been found that the location of the phase transition is only very little influenced by the value of \hat{g} . The influence of the imaginary part thus seems to be weak, at least as far as the location of the phase transition is concerned.

The simulation of the $SU(3)$ spin model is simplified by noting that the U 's can be diagonalized simultaneously for all sites of the lattice. The eigenvalues are given by $\exp(i\theta_l)$, $l = 1, 2, 3$, with $\theta_3 = -(\theta_1 + \theta_2)$. The partition function then reads

$$Z = \int \prod_x d\theta_{1x} d\theta_{2x} e^{-S_{\text{eff}}}, \quad (5)$$

where the effective action S_{eff} now contains an additional contribution from the Haar measure:

$$S_{\text{eff}} = S(\theta_{1x}, \theta_{2x}) - \sum_x \ln \left[\sin^2 \left(\frac{\theta_{1x} - \theta_{2x}}{2} \right) \sin^2 \left(\frac{2\theta_{1x} + \theta_{2x}}{2} \right) \sin^2 \left(\frac{\theta_{1x} + 2\theta_{2x}}{2} \right) \right]. \quad (6)$$

The Langevin equation for the effective action is then given by

$$\frac{d}{dt} \theta_{i,x} = - \frac{\partial S_{\text{eff}}}{\partial \theta_{i,x}} + \eta_{i,x}(t), \quad (7)$$

with η being a random-Gaussian-noise term,

$$\begin{aligned} \langle \eta_{i,x}(t) \rangle &= 0, \\ \langle \eta_{i,x}(t) \eta_{j,y}(t') \rangle &= 2\delta(t-t') \delta_{x,y} \delta_{i,j}. \end{aligned} \quad (8)$$

In the case of a complex action the phases θ_i will not stay real. The Langevin equation describes their time evolution in the complex plane. This corresponds to an analytic continuation of the original action, where U^\dagger has been replaced by U^{-1} . Notice that from the original $SU(3)$ variables the property $\det U = 1$ is preserved in this analytic continuation.

To simulate Eq. (7), we discretize the time derivative using a second-order Runge-Kutta scheme. This introduces systematic errors which are $O(\epsilon^3)$, ϵ being the discrete time step. To judge the reliability of the complex Langevin simulation, we first studied the limit $\beta = 0$ of the $SU(3)$ spin model. In this case the par-

tion function factorizes, and we are left with a single-site problem which is just the well-known $SU(3)$ one-link integral.¹⁶

We thus can compare the results obtained in the simulation with an exact solution. In Table I we show results obtained for $\langle \text{Tr}U \rangle$ and $\langle \text{Tr}U^{-1} \rangle$ for two different values of h and various chemical potentials. The Langevin averages are based on simulations with 1.5×10^6 iterations. We used a discrete time step $\epsilon = 0.005$. Obviously the expectation values agree well with the exact results, although they are systematically larger, which is probably because of the finite discrete time step used to integrate the Langevin equation. Even for the largest values of μ , where $\hat{g}/\hat{h} \approx 1$, we did not observe any instabilities. Thus even when the coupling strength of the complex part is comparable with that of the real part in the action the Langevin equation gives reliable results.

For $\beta \neq 0$ the results of the simulation cannot be compared with exact solutions. However, from the mean-field analysis and the limit $\beta = 0$ we expect that the results will differ only little from those of a con-

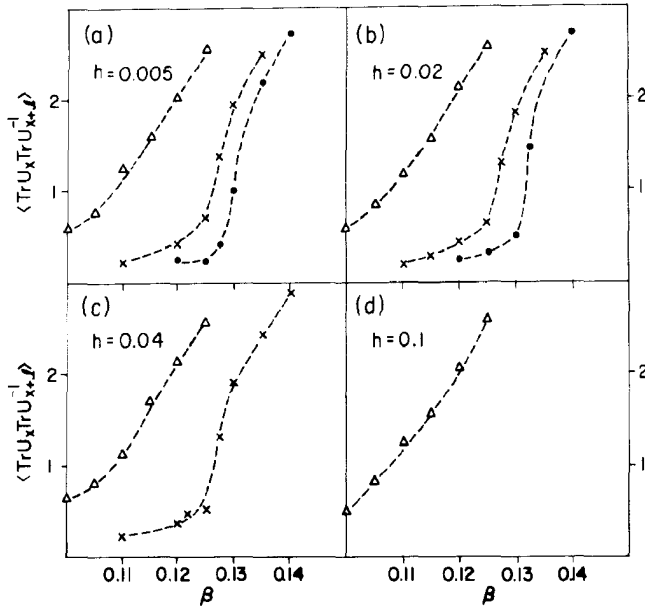


FIG. 1. Expectation value of the nearest-neighbor spin-spin correlation at nonzero μ for $h =$ (a) 0.005, (b) 0.02, (c) 0.04, and (d) 0.1. The symbols shown for the data correspond to fixed values of $\hat{h} = 0.025$ (circles), 0.05 (crosses), and 0.1365 (triangles). Curves are drawn to guide the eye. The data shown have been obtained on a 10^3 lattice averaging over 3000–6000 iterations.

ventional simulation with the same value of \hat{h} but $\hat{g} = 0$. We thus selected values of h and μ such that \hat{h} remains constant and compare these results with a conventional simulation with $\hat{g} = 0$, i.e., a real action. The results of the complex Langevin simulation are shown in Fig. 1, and those of a Langevin simulation with real action are shown in Fig. 2. Clearly for all three values of \hat{h} (0.025, 0.05, and 0.1365), graphs with the same value of \hat{h} agree within errors, and the change due to different values of \hat{g} is indeed small. They also agree well with the simulation of the “real action.” The results shown in Figs. 1 and 2 have been obtained on a 10^3 lattice with 3000–6000 iterations per

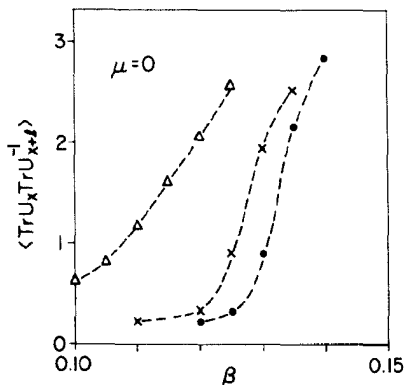


FIG. 2. Expectation value of the nearest-neighbor spin-spin correlation obtained from a Langevin simulation with a real action ($\hat{g} = 0$) for $\hat{h} = 0.025$ (circles), 0.05 (crosses), and 0.1365 (triangles) on a 10^3 lattice. Curves are drawn to guide the eye.

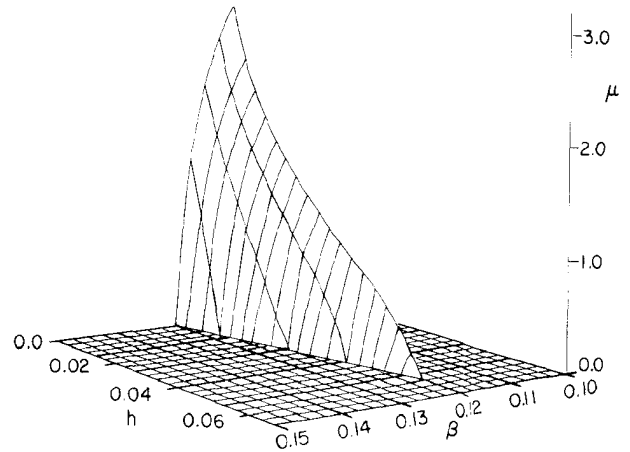


FIG. 3. Phase diagram of the SU(3) spin model at nonzero μ in the (β, h, μ) coupling space.

data point. Although we did not attempt to establish the existence of a first-order transition and the critical parameters for a second-order end point, our data are certainly consistent with the mean-field prediction. [As the transition in the SU(3) spin model, as in the Z(3) spin model, is only weakly first order, much larger lattices and better statistics would be necessary to determine the exact location of the transition.] The small deviations of the $\mu \neq 0$ simulation from those at $\mu = 0$ with the same value of \hat{h} indicate that the critical surface in the (β, h, μ) coupling space is well described by

$$(\beta_c, h_c, \mu_c) = (\beta_c, \hat{h}_c, 0), \tag{9}$$

where \hat{h}_c is the critical coupling at $\mu = 0$ and is related to h_c and μ_c through

$$\hat{h}_c = h_c \cosh \mu_c. \tag{10}$$

This phase diagram is shown in Fig. 3.

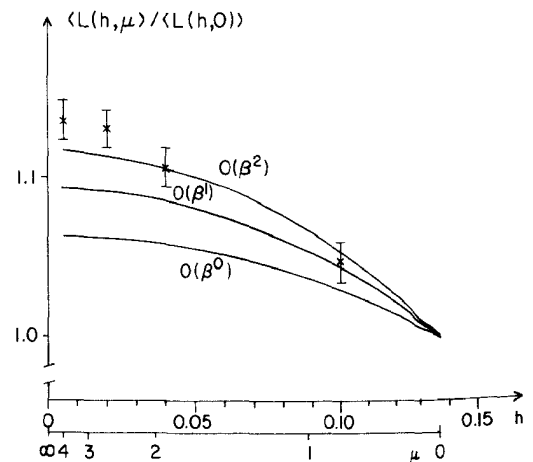


FIG. 4. Ratio of spin expectation value $L(h, \mu)/L(h, 0)$ at $\beta = 0.1$ and fixed $\hat{h} = 0.1365$. The data shown have been obtained on a 10^3 lattice. The curves show the three lowest-order contributions of a strong-coupling expansion for $L(h, \mu)/L(h, 0)$.

TABLE II. Strong-coupling expansion coefficients for $L(h, \mu) = \frac{1}{2} \langle \text{Tr} U_x + \text{Tr} U_x^{-1} \rangle$ for a fixed value of $\hat{h} = 0.1365$. The five values of (h, μ) tabulated correspond to the data points shown in Fig. 4.

| h | μ | $L_0(h, \mu)$ | $L_1(h, \mu)$ | $L_2(h, \mu)$ |
|--------|--------|---------------|---------------|---------------|
| 0.005 | 4 | 0.1550 | 1.1684 | 14.0440 |
| 0.02 | 2.5083 | 0.1548 | 1.1651 | 13.9983 |
| 0.04 | 1.8984 | 0.1542 | 1.1561 | 13.8750 |
| 0.1 | 0.8303 | 0.1500 | 1.0935 | 12.9981 |
| 0.1365 | 0 | 0.1457 | 1.0289 | 12.0812 |

To see the influence of the complex action on expectation values, we performed a high-statistics calculation at $\hat{h} = 0.1365$ and $\beta = 0.1$. In Fig. 4 we show results for the average spin

$$L(h, \mu) = \frac{1}{2} \langle \text{Tr} U_x + \text{Tr} U_x^{-1} \rangle, \quad (11)$$

normalized with the result for $\mu = 0$. The data are based on 20000 iterations on a 10^3 lattice. The results are compared with a strong-coupling expansion for the ratio $L(h, \mu)/L(h, 0)$, where

$$L(h, \mu) = L_0(h, \mu) + L_1(h, \mu)\beta + L_2(h, \mu)\beta^2 + \theta(\beta^3). \quad (12)$$

The expansion coefficients for some values of h and μ are given in Table II. Although the convergence of the strong coupling series is poor at $\beta = 0.1$ and $\hat{h} = 0.1365$, we find that it describes quite well the trend seen for the dependence on \hat{g} at fixed \hat{h} in the simulation. The influence of the imaginary part of the action also reflects itself in the difference of $\langle \text{Tr} U \rangle$ and $\langle \text{Tr} U^{-1} \rangle$. While in the $\mu = 0$ case $\langle \text{Tr} U \rangle = \langle \text{Tr} U^{-1} \rangle$, for $\mu \neq 0$ we find that $\langle \text{Tr} U^{-1} \rangle > \langle \text{Tr} U \rangle$. This is similar to what has been found from the analysis of the $\beta = 0$ limit (see Table I). $\langle \text{Tr} U \rangle$ ($\langle \text{Tr} U^{-1} \rangle$) is related to the free energy F_q ($F_{\bar{q}}$) of static fermion (antifermion) sources:

$$\langle \text{Tr} U \rangle \sim e^{-\beta F_q}, \quad (13)$$

$$\langle \text{Tr} U^{-1} \rangle \sim e^{-\beta F_{\bar{q}}}.$$

Thus the fact that $\langle \text{Tr} U^{-1} \rangle$ is larger than $\langle \text{Tr} U \rangle$ for $\mu \neq 0$ indicates that the free energy of static antifermions is smaller than that for static fermion sources, i.e., it is easier to screen the charge of the antifermion in a background of fermions created as a result of nonzero values of μ .

To summarize, we find that the SU(3) spin model with nonzero chemical potential can be well simulated with a complex Langevin algorithm. Even for large values of the chemical potential the algorithm converges. This is encouraging for attempts to simulate

QCD at finite density by this approach. Work in this direction is in progress. The phase diagram that we obtain from the simulation of a complex action with $\mu \neq 0$ is obviously closely related to that of the $\mu = 0$ real action with a suitably adjusted external-field parameter h . This is expected to be the case also for lattice QCD in the strong-coupling, large-fermion-mass limit, where the SU(3) spin model is a good approximation. Attempts to reinterpret existing $\mu = 0$ data under this assumption have been undertaken recently.¹⁷

We thank S. Duane and J. Polonyi for many valuable discussions. This work was supported in part by the National Science Foundation through Grant No. PHY82-01948.

¹F. Fucito, C. Rebbi, and S. Solomon, Nucl. Phys. **B248**, 615 (1984), and Phys. Rev. D **31**, 1461 (1985); J. Polonyi, H. W. Wyld, J. B. Kogut, J. Shigemitsu, and D. K. Sinclair, Phys. Rev. Lett. **53**, 644 (1984); R. V. Gavai, M. Lev, and B. Peterson, Phys. Lett. **140B**, 367 (1984), and **149B**, 492 (1984); R. V. Gavai and F. Karsch, University of Illinois Report No. ILL-(TH)-85-#19, April 1985 (to be published).

²F. Fucito, R. Kinney, and S. Solomon, California Institute of Technology Report No. CALT-68-1189, October 1984 (to be published).

³J. B. Kogut, J. Polonyi, H. W. Wyld, and D. K. Sinclair, Phys. Rev. Lett. **54**, 1475 (1985).

⁴P. Hasenfratz and F. Karsch, Phys. Lett. **125B**, 308 (1983); J. Kogut, H. Matsuoka, M. Stone, H. W. Wyld, S. Shenkar, J. Shigemitsu, and D. K. Sinclair, Nucl. Phys. **B225[FS9]**, 93 (1983); N. Bilic and R. V. Gavai, Z. Phys. C **23**, 77 (1984).

⁵A. Nakamura, Phys. Lett. **149B**, 391 (1984).

⁶G. Parisi, Phys. Lett. **131B**, 393 (1983).

⁷J. R. Klauder, "Stochastic Quantization," Lectures given at the XXII Schlading School, March 1983 (unpublished).

⁸J. R. Klauder, Acta Phys. Austriaca, Suppl. **25**, 251 (1983), and Phys. Rev. A **29**, 2036 (1984); J. R. Klauder and W. R. Petersen, J. Stat. Phys. **39**, 53 (1985).

⁹E. Gozzi, Phys. Lett. **150B**, 119 (1985).

¹⁰H. W. Hamber and Hai-cang Ren, Phys. Lett. **159B**, 330 (1985).

¹¹J. Ambjorn, M. Flensburg, and C. Peterson, Phys. Lett. **159B**, 335 (1985).

¹²T. Banks and A. Ukawa, Nucl. Phys. **B225[FS9]**, 145 (1983).

¹³J. Bartholomew, D. Hochberg, P. H. Damgaard, and M. Gross, Phys. Lett. **133B**, 218 (1983).

¹⁴F. Green and F. Karsch, Nucl. Phys. **B238**, 297 (1984).

¹⁵C. DeTar and T. DeGrand, Nucl. Phys. **B225[FS9]**, 590 (1983).

¹⁶F. Green and S. Samuel, Nucl. Phys. **B190[FS3]**, 113 (1981); J. B. Kogut, M. Snow, and M. Stone, Nucl. Phys. **B200[FS4]**, 211 (1982); K. E. Eriksson, N. Svartholm, and B. S. Skagerstam, J. Math. Phys. **22**, 2276 (1981).

¹⁷J. Engels and H. Satz, Phys. Lett. **159B**, 151 (1985).